Microscopic method for $E0$ transition matrix elements

B. A. Brown,[1] A. B. Garnsworthy,[2] T. Kibédi,[3] and A. E. Stuchbery[3]

[1]*Department of Physics and Astronomy and National Superconducting Cyclotron Laboratory Michigan State University,
East Lansing, Michigan 48824-1321, USA*

[2]*Physical Sciences Division, TRIUMF, 4004 Wesbrook Mall, Vancouver, British Columbia, Canada V6T 2A3*

[3]*Department of Nuclear Physics, Research School of Physics and Engineering, Australian National University,
Canberra, Australian Capital Territory 2601, Australia*

We present a microscopic model for electric monopole ($E0$) transition matrix elements by combining a configuration interaction model for orbital occupations with an energy-density functional model for the single-particle potential and radial wave functions. The configuration interaction model is used to constrain the orbital occupations for the diagonal and off-diagonal matrix elements. These are used in an energy-density functional calculation to obtain a self-consistent transition density. This density contains the valence contribution, as well as the polarization of the protons by the valence protons and neutrons. We show connections between $E0$ matrix elements and isomer and isotope shifts of the charge radius. The spin-orbit correction to the charge density is important in some cases. This model accounts for a large part of the data over a wide region of the nuclear chart. It also accounts for the shape of the observed electron scattering form factors. The results depend on the Skyrme parameters used for the energy-density functional and might be used to provide new constraints for them.

Introduction. Electric monopole ($E0$) transitions between spin-zero states in atomic nuclei were first suggested by Gamow [1] when interpreting a mysterious electron line in the β-decay spectrum of radon [2]. Single-photon $0 \rightarrow 0$ transitions are strictly forbidden. $E0$ transitions can only proceed via internal conversion, electron-positron pair conversion, or very rarely by double-photon emission. $E0$ transitions between the first excited 0^+ state and the 0^+ ground state are one of the dominant features of the low-energy nuclear structure of even-even nuclei. The total $E0$ transition probability, $W(E0) = \Omega(E0)\, \rho^2(E0)$, for a transition between the initial and final states, $|i\rangle$ and $|f\rangle$, conveniently can be separated into electronic, $\Omega(E0)$, and nuclear, $\rho(E0)$, factors. The quantity $\rho(E0)$ is the dimensionless monopole transition strength, carrying all the information about the nuclear structure, and is related to the monopole matrix element, $M(E0)$, by

$$\rho(E0) = \langle f|M(E0)|i\rangle/(eR^2), \qquad (1)$$

where R is the nuclear radius in fm defined by $R = 1.2A^{1/3}$. The operator is $M(E0) = r^2 \equiv e\sum_i r_i^2$, where the sum is over all protons in the nucleus. It is widely accepted that $E0$ transitions provide sensitive tests [3] of various nuclear structure models for understanding volume oscillations, isotope and isomer shifts, and, in particular, nuclear shape coexistence [4].

In recent years there has been a resurgence in the number of measurements of $E0$ transition strengths encouraged by their association with shape coexistence. There are relatively few $E0$ transition strengths known experimentally, mainly due to the challenging nature of the necessary parent lifetime and $E0$ branching ratio measurements. Although a lifetime measurement can be made by detecting a competing γ-ray branch, a range of experimental techniques are necessary as the lifetimes of the parent state can vary from femtoseconds to hundreds of nanoseconds. The branching ratio must come from electron spectroscopy which can be hindered by the

relatively low emission intensities, in comparison to γ-ray emission, in addition to large backgrounds, especially during in-beam measurements. Nevertheless, there are now a number of experimental setups becoming available worldwide that are bringing new concepts and modern equipment to face these challenges [5–10]. With renewed interest and renewed capabilities, it is expected that the number of experimentally measured $E0$ transition strengths will dramatically increase over the next several years.

Previous calculations of $E0$ transition strengths are mostly based on collective models and shape coexistence [3,4,11–15]. In this paper we present a theoretical model for $E0$ matrix elements based on a combination of configuration interaction (CI) results in a spherical basis for orbital occupations, together with energy-density functional (EDF) calculations for the monopole core polarization. This core polarization is caused by the change in the nodal structure of the radial wave functions for the orbitals that participate in the valence transition. The core polarization is not proportional to the valence $E0$ matrix element.

Previous models starting with a spherical basis are based on two-level models, e.g., Refs. [16,17], and others reviewed in Ref. [3]. Our method is a generalization of the two-level model and makes connections to isomer and isotope shifts via a common EDF approach. We choose several cases across the nuclear chart for which good wave functions with CI methods can be obtained and for which there are rather precise experimental data on $E0$ matrix elements. We start with the case of ^{90}Zr for which a two-level model for the two 0^+ states is a good approximation and make a connection to the observed isomer shift (the change in the charge radius between the isomeric excited state and the ground state) for ^{89}Y. Then we proceed to the cases of ^{206}Pb and ^{68}Ni that are determined by a CI space with valence neutrons. Finally, we show results for the more complicated cases of ^{26}Mg,

^{32}S, and ^{58}Ni where both valence protons and neutrons are involved.

Application to a two-level model for ^{90}Zr. Our discussion for ^{90}Zr is similar to previous results based on a two-level model summarized in Ref. [3]. However, it will be used to formulate a more general approach for the CI method and its connection to EDF results. In the shell model these two 0^+ states are dominated by the mixing of the configurations

$$|a\rangle = |C_a,(1p_{1/2})^2\rangle$$

and

$$|b\rangle = |C_b,(0g_{9/2})^2\rangle, \tag{2}$$

where C represents the ^{88}Sr closed-shell configuration for neutrons up to $N = 50[0s_{1/2}^2, 0p_{3/2}^4, 0p_{1/2}^2, 0d_{5/2}^6, 0d_{3/2}^4, 1s_{1/2}^2, 0f_{7/2}^8, 0f_{5/2}^6, 1p_{3/2}^4, 1p_{1/2}^2, 0g_{9/2}^{10}]$ and for protons up to $Z = 38 [0s_{1/2}^2, 0p_{3/2}^4, 0p_{1/2}^2, 0d_{5/2}^6, 0d_{3/2}^4, 1s_{1/2}^2, 0f_{7/2}^8, 0f_{5/2}^6, 1p_{3/2}^4]$. The proton ($q = p$) and neutron ($q = n$) radial densities of these two configurations are given by

$$\rho_{qx}(r) = \sum_k O_{qxk}\,\psi_{qxk}^2(r), \tag{3}$$

where $x = a/b$ and $k = (n,\ell,j)$ are the quantum numbers for the spherical single-particle wave functions, $\psi_{qxk}(r)[Y^{(\ell)}(\hat r) \otimes \chi^{(s)}]^{(j)}$. The O are the orbital occupations. In this case $O_k = (2j + 1)$ for the filled neutrons up to $N = 50$ and for the filled protons up to $Z = 38$. The occupations are zero for all other orbitals except $O_{pa,1p_{1/2}} = 2$ and $O_{pb,0g_{g/2}} = 2$. The sum over k is for the 11 orbitals given above.

In the simplest model the radial wave functions, ψ, only depend on k, and the core wave functions C_a and C_b are the same. However, in the EDF model ψ also depends on q as well as a and b since the different orbital occupancies lead to different self-consistent potentials and slightly different radial wave functions for the orbitals in the core C_a and C_b.

The volume integral of Eq. (3) is (Z/N) for $q = (p/n)$. The matrix element of the $E0$ operator for protons is

$$\int \rho_{px}r^2\,d\tau = \langle x|r^2|x\rangle_p = \sum_k O_{pxk}\,\langle pxk|r^2|pxk\rangle. \tag{4}$$

In the two-level model these two proton configurations are mixed:

$$|0_1^+\rangle = \alpha|a\rangle + \beta|b\rangle$$

and

$$|0_2^+\rangle = \beta|a\rangle - \alpha|b\rangle, \tag{5}$$

with $\beta = \pm\sqrt{1 - \alpha^2}$.

With maximal mixing, $\alpha = \beta = 1/\sqrt{2}$, the r^2 matrix elements are

$$\langle 0_1^+|r^2|0_1^+\rangle = \langle 0_2^+|r^2|0_2^+\rangle = \tfrac{1}{2}[\langle b|r^2|b\rangle + \langle a|r^2|a\rangle]$$
$$= \tfrac{1}{2}\langle C_b|r^2|C_b\rangle + \tfrac{1}{2}\langle C_a|r^2|C_a\rangle$$
$$+ \langle 0g_{9/2}|r^2|0g_{9/2}\rangle + \langle 1p_{1/2}|r^2|1p_{1/2}\rangle \tag{6}$$

and

$$\langle 0_1^+|r^2|0_2^+\rangle = \tfrac{1}{2}[\langle b|r^2|b\rangle - \langle a|r^2|a\rangle]$$
$$= \tfrac{1}{2}\langle C_b|r^2|C_b\rangle - \tfrac{1}{2}\langle C_a|r^2|C_a\rangle$$
$$+ \langle 0g_{9/2}|r^2|0g_{9/2}\rangle - \langle 1p_{1/2}|r^2|1p_{1/2}\rangle. \tag{7}$$

(The sign of the off-diagonal matrix element is not determined, but experiment depends only on its square.) In the harmonic oscillator (HO) model for the radial wave functions, the core term cancels and the $E0$ matrix element is given by

$$\langle 0_1^+|r^2|0_2^+\rangle = \tfrac{11}{2}b^2 - \tfrac{9}{2}b^2 = b^2, \tag{8}$$

where $b^2 = \frac{\hbar}{m\omega}$. With $\hbar\omega = 45A^{-1/3} - 25A^{-2/3}$, $b^2 = 4.71$ fm^2. Taking into account the finite charge size and the relativistic contributions [18] for the protons and neutrons, the charge matrix element for the $E0$ transition is $\langle 0_1^+|r^2|0_2^+\rangle_{ch} = 5.32$ fm^2 (the increase is mainly due to the spin-orbit contribution). This is much larger than the experimental value of 1.70(3) [19]. This discrepancy was noted in the experimental lifetime paper [17] where they used $\alpha = 0.80$ and $\beta = 0.60$.

This $E0$ matrix element is closely connected to the isomer shift between the $1/2^-$ ground state and $9/2^+$ excited state of ^{89}Y that has been measured to be $\delta\langle r^2\rangle_{ch} = 0.84(8)$ fm^2 [20]. In the single-particle model the isomer shift is given by

$$\delta\langle r^2\rangle = \langle C_b',0g_{9/2}|r^2|C_b',0g_{9/2}\rangle - \langle C_a',1p_{1/2}|r^2|C_a',1p_{1/2}\rangle$$
$$= \langle C_b'|r^2|C_b'\rangle - \langle C_a'|r^2|C_a'\rangle$$
$$+ \langle 0g_{9/2}|r^2|0g_{9/2}\rangle - \langle 1p_{1/2}|r^2|1p_{1/2}\rangle, \tag{9}$$

where C' represents the ^{88}Sr closed-shell configuration for ^{89}Y. The orbital configurations for C and C' are the same, but the self-consistent EDF solutions for ^{90}Zr and ^{89}Y, respectively, are different. With HO radial wave functions the core terms cancel, and the value for the difference in charge radii is given by Eq. (8). Together with the spin-orbit contribution this gives $\delta\langle r^2\rangle_{ch} = 5.31$ fm^2. Thus, in the limit of maximal mixing for ^{90}Zr, $E0$ matrix element and ^{89}Y isomer shift are the same in the HO model and are both are a factor of three to four larger than experimental results.

Next we replace the HO radial wave functions with those obtained from self-consistent EDF calculations carried out with the Skyrme form for the functional. We start with the Skyrme parameter set *Skx* [21]. The EDF results obtained for a closed-shell configuration for ^{88}Sr plus one proton in the $1p_{1/2}$ orbital for the $1/2^-$ ground state and one proton in the $0g_{9/2}$ orbital for the $9/2^+$ excited state of ^{89}Y are given in Table I. The resulting isomer shift of the charge radii is now in much better agreement with experimental results. The difference in the charge radii of the valence orbitals $\langle 0g_{9/2}|r^2|0g_{9/2}\rangle - \langle 1p_{1/2}|r^2|1p_{1/2}\rangle = 4.81$ fm^2, is slightly reduced from the HO model value of 5.31 fm^2, but the isomer shift (the observable) is reduced to 0.82 fm^2 due to a cancellation coming from the $\langle C_b'|r^2|C_b'\rangle - \langle C_a'|r^2|C_a'\rangle$ term in Eq. (9). This is due to a self-consistent rearrangement of all protons as a response to the added density of the valence proton. Qualitatively, this is due to the interior density for the $1p$ orbital that forces the proton density to be pushed out in order to achieve self-consistent saturation for the interior density. From Eq. (9), the total isomer

TABLE I. Matrix elements in units of fm^2. For ^{89}Y we give $\delta\langle r^2\rangle_{ch}$, and for the others we give $|\langle 0_f^+|r^2|0_1^+\rangle|_{ch}$, where f is given in the second column. The spin-orbit contribution given in column 5 is included in the other theory results. Results are given for the single-particle (SP), two-level (TL), and configuration interaction (CI) models discussed in the text. For the two state mixing ^{58}Ni the matrix elements are added in quadrature.

	f	exp	Model	Spin	EDF valence	EDF valence plus core		Ratios		
				orbit	(Skx)	(Skx)	$(s3)$			
		a			b	c	d	a/b	a/c	a/d
^{89}Y		0.84(8) [20]	SP	0.61	4.81	0.82	0.34	0.17	1.02	2.47
			CI	0.51	4.54	0.97	0.60	0.19	0.9	1.5
^{90}Zr	2	1.70(3) [19]	TL	0.61	4.71	0.71	0.36		2.4	5.2
			CI	0.53	4.48	0.90	0.57	0.4	1.9	3.0
^{206}Pb	2	1.72(6) [19]	CI	-0.04	-0.04	0.66	1.43	43	2.6	1.2
^{68}Ni	2	1.41(3) [23]	CI	0.43	0.43	1.06	0.74	3.3	1.3	1.9
^{58}Ni	2	0.054(14) [19]	CI	0.33	0.30	1.47	1.80			
	3	5.5(10) [24]	CI	-0.08	1.01	1.69	2.62			
	2 + 3	5.5(10) [24]	CI		1.05	2.23	3.18	5.2	2.5	1.7
^{32}S	3	2.0(3) [19]	CI	-0.04	0.11	0.74	1.06	18	2.7	1.9
^{26}Mg	2	3.5(12) [24]	CI	0.16	0.26	0.93	1.11	13	3.8	3.2
^{26}Mg	3	3.8(10) [24]	CI	0.00	0.61	1.40	1.79	6.2	2.7	2.1

shift can be written as a sum of three terms, the change in the core radius, the difference in the valence point proton radii, and the spin-obit contribution from the change in the valence orbitals: $\delta\langle r^2\rangle = -3.99 + 4.20 + 0.61 = 0.82 \text{ fm}^2$.

For the ^{90}Zr $E0$ transition we carried out EDF calculations for the configurations of Eq. (2) and then used these in Eq. (7) for the $E0$ matrix element. The response of the core to two valence protons is approximately two times that for one valence proton; hence, the connection between the core terms in Eqs. (7) and (9) is

$$\langle C_b|r^2|C_b\rangle - \langle C_a|r^2|C_a\rangle = 2(\langle C_b'|r^2|C_b'\rangle - \langle C_a'|r^2|C_a'\rangle). \tag{10}$$

In analogy with the isomer shift, the $E0$ matrix element can be written as a sum of three terms: $\langle 0_1^+|r^2|0_2^+\rangle = -4.00 + 4.10 + 0.61 = 0.71 \text{ fm}^2$. This is reduced compared to HO due to the change in the core radius. The results are slightly different from those of the isomer shift due to the small mass dependence of the valence radii in the EDF calculation.

Application for configuration-interaction models. The final step is to use EDF together with the orbital occupations from large-basis CI calculations. There will be many configurations analogous to those of Eq. (2). For a given pair of eigenstates $|1\rangle$ and $|2\rangle$, one can calculate the diagonal occupations for protons ($q = p$) and neutrons ($q = n$) for orbitals k,

$$O_{q1k} = \langle 1|[a_{qk}^+ \otimes \tilde{a}_{qk}]^{\lambda=0}|1\rangle \tag{11}$$

and

$$O_{q2k} = \langle 2|[a_{qk}^+ \otimes \tilde{a}_{qk}]^{\lambda=0}|2\rangle, \tag{12}$$

as well as the off-diagonal occupation change

$$O_{q12k}' = \langle 1|[a_{qk}^+ \otimes \tilde{a}_{qk}]^{\lambda=0}|2\rangle. \tag{13}$$

(The sum over k for O_{q12k}' is zero.) To use these in EDF calculations we take the average of O_{q1k} and O_{q2k} and then

add and subtract the one-half of the off-diagonal term to make two derived sets of occupations a and b:

$$O_{qak} = \tfrac{1}{2}[O_{q1k} + O_{q2k} - O_{q12k}'] \tag{14}$$

and

$$O_{qbk} = \tfrac{1}{2}[O_{q1k} + O_{q2k} + O_{q12k}']. \tag{15}$$

These, together with the $(2j + 1)$ occupations of the filled orbitals, are used in Eq. (3) to construct the densities for a and b. The difference of the two densities $\rho_{pb}(r) - \rho_{pa}(r)$ gives the proton radial transition density for the $E0$ transition. In the HO limit the diagonal terms cancel and the transition density only comes from the off-diagonal term determined by O'. When these constrained densities are used in EDF calculations, the core response is taken into account by the change in the diagonal terms induced by O'.

With this procedure we reproduce the EDF result discussed above for ^{90}Zr. We propose to use this method for other $E0$ transitions that can be calculated within the CI method. Here we use these results for $E0$ transitions that connect to the 0^+ ground state. But the method is general and can be applied to any J^π and to transitions between excited states.

For ^{89}Y and ^{90}Zr we use the $j4$ model space for the $(0f_{5/2}, 1p_{3/2}, 1p_{1/2}, 0g_{9/2})$ set of orbitals. The wave functions are obtained with the $jj44pna$ Hamiltonian [22]. We calculate the CI occupations for the two states of interest, O_{q1k} and O_{q2k}, and use these to constrain the orbital occupations for the EDF calculation as discussed above. The $j4$ results for ^{89}Y given in Table I are similar to those of the single-particle model. For the ^{90}Zr $E0$ transition the off-diagonal occupations for protons O_{p12k}' [$q = p$ in Eq. (13)] are 0.946 ($0g_{9/2}$), -0.747 ($1p_{1/2}$), -0.150 ($1p_{3/2}$), and -0.049 ($0f_{5/2}$).

We use these constrained orbital occupations for the EDF calculations to obtain self-consistent radial densities, $\rho(r)_{qa}$ and $\rho(r)_{qb}$. The proton transition density is given by
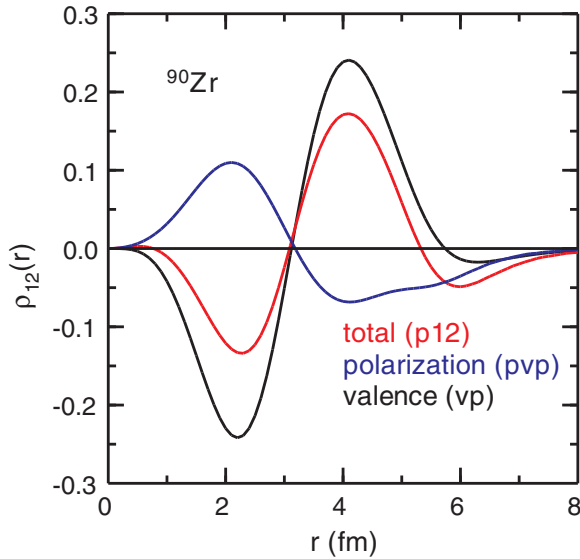
$$\rho_{p12}(r) = \rho_{pb}(r) - \rho_{pa}(r). \tag{16}$$

FIG. 1. Calculated proton transition densities for ^{90}Zr obtained with the *Skx* energy-density functional. Contributions are shown for the three terms in Eq. (17).

FIG. 2. Calculated form factors for ^{26}Mg. The dashed lines are for the valence space contribution only. The solid lines take into account the valence space and the core polarization.

We can calculate the transition density coming just from the valence protons density, $\rho_{vp}(r)$. If we subtract this from the total proton transition density, $\rho_{p12}(r)$, we have the contribution coming from the change of the proton density induced by the change in the valence proton density, $\rho_{pvp}(r)$. Thus the total can be understood as a sum of two terms:

$$\rho_{p12}(r) = \rho_{vp}(r) + \rho_{pvp}(r). \tag{17}$$

These densities for ^{90}Zr are shown in Fig. 1. If all O_{q12k} are zero then the $E0$ matrix element is zero.

Next we apply our method to a variety of other cases across the nuclear chart: ^{206}Pb in the $(0h_{9/2}, 1f_{7/2}, 1f_{5/2}, 2p_{3/2}, 1p_{1/2}, 0i_{13/2})$ model space for neutrons with the modified Kuo-Herling Hamiltonian [25]; ^{68}Ni in the $j4$ model space for neutrons with the $jj44pna$ Hamiltonian [22]; ^{58}Ni in the $(1p, 0f)$ model space for protons and neutrons with the GPFX1A Hamiltonian [26]; and ^{26}Mg in the $(1s, 0d)$ model space for protons and neutrons with the USDB Hamiltonian [27]. The calculations were carried out with the code NUSHELLX [28]. For all cases considered here, the calculated energy of the excited state is within 200 keV of the experimental value. The results are given in Table I. For ^{206}Pb and ^{68}Ni only neutrons are active and the contribution from the model space is zero (except for the spin-orbit contribution coming from the neutrons). The proton contribution for the $E0$ matrix element comes entirely from the polarization of the protons from the valence neutrons $[\rho(r)_{cpvn}]$. Our results for ^{206}Pb are similar to the two-level model of Zamick [16]; the dominant orbitals in the transition are $1f_{5/2}$ and $2p_{1/2}$. The $E0$ transition strength is related to the isotope shifts of ^{204,207}Pb relative to ^{208}Pb related to these two orbitals. The density dependence of the interaction that gives rise to the core polarization is important [29], and in our approach this is provided by the Skyrme interaction.
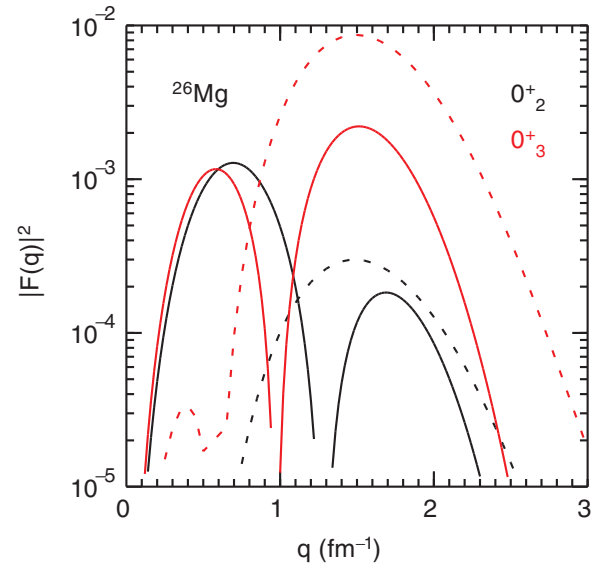
Finally we consider ^{26}Mg, ^{32}S, and ^{58}Ni. For ^{26}Mg and ^{58}Ni there is additional information on the transition form factors from inelastic electron scattering [24]. ^{32}S provides a test of our model for a nucleus with equal number or protons and neutrons. The $E0$ matrix elements are zero in the sd and pf model spaces with harmonic-oscillator radial wave-function approximation since all of the valence $\langle r^2 \rangle$ matrix elements are the same. But the valence proton transition densities are not zero and this provides the mechanism for proton core polarization involving both valence protons (pvp) and valence neutrons (pvn):

$$\rho_{p12}(r) = \rho_{vp}(r) + \rho_{pvp}(r) + \rho_{pvn}(r). \tag{18}$$

In Ref. [24] the strength and shape of the form factors were explained by adding an arbitrary small amount of $0d_{5/2} \rightarrow 1d_{5/2}$ and $0f_{7/2} \rightarrow 1f_{7/2}$ to the off-diagonal CI transition density for ^{26}Mg and ^{58}Ni, respectively. These are part of the giant monopole transition densities. Our core polarization model can be represented as an addition of the giant monopole transition density with an amplitude that is determined by the Skyrme parameters. We can calculate the form factor $F(q)$ coming from the $j_0(qr)$ integral of Eq. (16). The results for $|F(q)|^2$ are shown in Fig. 2. The valence contribution is in agreement with those given in Ref. [24]. The shape for the total form factor is in reasonable agreement with the data given in Ref. [24]; however, its magnitude around $q = 0.6$ fm^{-1} is two orders of magnitude larger than the valence contribution, but it is still about an order of magnitude smaller than the data at low q, reflecting the fact that the $E0$ matrix elements are about a factor of three smaller than experiment (Table I). We will discuss the possible reason for this disagreement below.

The calculated $E0$ matrix element for the 0_2^+ state at 2.942 MeV in ^{58}Ni is much larger than the experimental value. Also the calculated $E2$ matrix element for the $0_1^+ \to 2_2^+$ of 13.0 e fm^2 is much larger than the experimental value of 1.4(5) e fm^2 for the 2_2^+ state at 2.775 MeV. The minimal resolution of both of these problems requires a remixing of the theoretical 0_2^+ and 2_2^+ states with the 0_3^+ and 2_3^+ states that lie about 0.4 MeV higher. After remixing to give the small $E0$ to the 0_2^+ state, the value for the 0_3^+ state is 3.2 fm^2 with EDF($s3$), about half of the experimental value. It remains to be seen how (or if) the GPFX1A Hamiltonian can be modified to explain these small matrix elements.

We have explored the sensitively to the Skyrme parameters by using the 18 parameter sets that go with Table I Ref. [30]. Of these 18, the KDE0v1 ($s3$) set gives the largest difference for the r^2 matrix elements compared to Skx (the dependence on m_n^*/m is small). Part of this is correlated with the nuclear matter incompressibility that is larger for Skx ($K_m = 270$ MeV) compared to $s3$ ($K_m = 220$ MeV). For ^{206}Pb $s3$ gives a much larger core polarization than the other sets given in Table I of Ref. [30]. This is correlated with the t_2 parameter that is much larger in $s3$ compared to the others. The full dependence on the Skyrme parameters remains to be explored and perhaps exploited as an additional constraint.

The core polarization is caused by the change in the nodal structure of the radial wave functions for the orbitals that participate in the valence transition. There is a connection with the isomer and isotope shifts in the nuclear charge radii. EDF calculations can only account for part of the observed isotope shift. For example, recent results for ^{49,51,52}Ca [31] show a rapid increase in the r^2 charge radius beyond $N = 28$ for which only about half is accounted for by the EDF calculations [31,32]. Some of the isotope shift anomalies can be accounted for by quadrupole zero-point motion corrections. This correction arises from second-order configuration admixtures of the type $[2_{\text{valence}}^+ \otimes 2_{\text{collective}}^+]^{J=0^+}$. One may need an expansion of the model space to include octupole correlations to account for the increase in radii beyond $N = 28$. These second-order corrections will also be important for the $E0$ matrix elements, and the next step for future work will be to calculate their contribution.

Conclusions. In conclusion, we have presented a microscopic model for electric monopole ($E0$) transition matrix elements that can be used with orbital occupations obtained from CI calculations. The most important part of the CI Hamiltonian is the pairing part ($J = 0$, $T = 1$) that provides the mixing required for the nonzero off-diagonal orbital occupations. These occupations are used as constraints for an EDF calculation that is used to obtain a self-consistent transition density. We discussed the connections between $E0$ matrix elements and isomer and isotope shifts of the charge radius. We also showed that the electromagnetic spin-orbit correction to the charge density is important in some cases. For the nuclei considered here, this model accounts for a large part of the data over a wide region of the nuclear chart. The ratio of the experimental matrix element divided by the conventional valence EDF matrix element is shown in Table I by the ratio a/b; it ranges from 0.2 to 43. This a greatly improved with the valance-plus-core model where the ratios a/c (Skx) and a/d (s3) are reduced to the range 1 to 5. About half of this comes from the uncertainties in Skyme EDF functional. Overall the experimental matrix elements are about a factor of two larger than theory, indicating the need for an effective charge that can come from a second-order correction. The model can be applied to $E0$ transitions between any J^π states. It also accounts for the shape of the observed electron scattering form factors. As demonstrated for the case of ^{58}Ni, comparison of experiment to our model results provide tests of the wave functions and Hamiltonians used for the CI method. The results depend on the Skyrme parameters used for energy-density functional and might be used to provide new constraints for these parameters.

[1] G. Gamow, *Constitution of Atomic Nuclei and Radioactivity* (Clarendon Press, Oxford, 1931).

[2] C. D. Ellis, Proc. R. Soc. London, Ser. A **129**, 180 (1930).

[3] J. L. Wood, E. F. Zganjar, C. De Coster, and K. Heyde, Nucl. Phys. A **651**, 323 (1999).

[4] K. Heyde and J. L. Wood, Rev. Mod. Phys. **83**, 1467 (2011).

[5] J. M. Regisa, H. Mach, G. S. Simpson, J. Jolie, G. Pascovici, N. Saed-Samii, N. Warr, A. Bruce, J. Degenkolb, L. M. Fraile, C. Fransen, D. G. Ghita, S. Kisyov, U. Koester, A. Korgul, S. Lalkovski, N. Mărginean, P. Mutti, B. Olaizola, Z. Podolyák, P. H. Regan, O. J. Roberts, M. Rudigier, L. Stroe, W. Urban, and D. Wilmsen, Nucl. Instrum. Methods Phys. Res. A **726**, 191 (2013).

[6] T. Kibédi, A. E. Stuchbery, G. D. Dracoulis, and K. A. Robertson, EPJ Web Conf. **35**, 06001 (2012).

[7] N. Larson, S. N. Liddick, M. Bennett, A. Bowe, A. Chemey, C. Prokop, A. Simon, A. Spyrou, S. Suchyta, S. J. Quinn, S. L. Tabor, P. L. Tai, V. Tripathi, and J. M. VonMoss, Nucl. Instrum. Methods Phys. Res. A **727**, 59 (2013).

[8] S. Ketelhut, L. J. Evitts, A. B. Garnsworthy, C. Bolton, G. C. Ball, R. Churchman, R. Dunlop, G. Hackman, R. Henderson, M. Moukaddam, E. T. Rand, C. E. Svensson, and J. Witmer, Nucl. Instrum. Methods Phys. Res. A **753**, 154 (2014).

[9] J. Pakarinen, P. Papadakis, J. Sorri, R.-D. Herzberg, P. T. Greenlees, P. A. Butler, P. J. Coleman-Smith, D. M. Cox, J. R. Cresswell, P. Jones, R. Julin, J. Konki, I. H. Lazarus, S. C. Letts, A. Mistry, R. D. Page, E. Parr, V. F. E. Pucknell, P. Rahkila, J. Sampson, M. Sandzelius, D. A. Seddon, J. Simpson, J. Thornhill, and D. Wells, Eur. Phys. J. A **50**, 53 (2014).

[10] P. Papadakis, J. Pakarinen, P. A. Butler, D. M. Cox, P. Davies, P. Greenlees, R.-D. Herzberg, M. Huyse, D. G. Jenkins, J. Konki, G. G. O'Neill, P. Rahkila, K. Ranttila, V-P. Saarela, J. Thornhill, P. Van Duppen, and D. Wells, JPS Conf. Proc. **6**, 030023 (2015).

[11] J. O. Rasmussen, Nucl. Phys. **19**, 85 (1960).

[12] J. Kantele, R. Julin, M. Luontama, A. Passoja, and T. Poikolainen, Z. Phys. A **289**, 157 (1979).

[13] B. G. Carlsson, J. Toivanen, and A. Pastore, Phys. Rev. C **86**, 014307 (2012).

[14] Z. P. Li, T. Nikŭić, and D. Vretenar, J. Phys. G: Nucl. Part. Phys. **43**, 024005 (2016).

[15] K. Matsuyanagi, M. Matsuo, T. Nakatsukasa, K. Yoshida, N. Hinohara, and K. Sato, J. Phys. G: Nucl. Part. Phys. **43**, 024006 (2016).

[16] J. W. Tape, E. G. Adelberger, D. Burch, and L. Zamick, Phys. Rev. Lett. **29**, 878 (1972).

[17] D. Burch, P. Russo, H. Swanson, and E. G. Adelberger, Phys. Lett. B **40**, 357 (1972).

[18] W. Bertozzi, J. Friar, J. Heisenberg, and J. W. Negele, Phys. Lett. B **41**, 408 (1972).

[19] T. Kibédi and R. H. Spear, At. Data Nucl. Data Tables **89**, 77 (2005).

[20] B. Cheal, M. D. Gardner, M. Avgoulea, J. Billowes, M. L. Bissell, P. Campbell, T. Eronen, K. T. Flanagan, D. H. Forest, J. Huikari, A. Jokinen, B. A. Marsha, I. D. Moorec, A. Nieminena, H. Penttilä, S. Rinta-Antila, B. Tordoff, G. Tungate, and J. Äystö, Phys. Lett. B **645**, 133 (2007).

[21] B. A. Brown, Phys. Rev. C **58**, 220 (1998).

[22] A. F. Lisetskiy, B. A. Brown, M. Horoi, and H. Grawe, Phys. Rev. C **70**, 044314 (2004).

[23] S. Suchyta, S. N. Liddick, Y. Tsunoda, T. Otsuka, M. B. Bennett, A. Chemey, M. Honma, N. Larson, C. J. Prokop, S. J. Quinn, N. Shimizu, A. Simon, A. Spyrou, V. Tripathi, Y. Utsuno, and J. M. VonMoss, Phys. Rev. C **89**, 021301(R) (2014).

[24] H. Blok, H. P. Blok, J. F. A. van Hienen, G. van der Steenhoven, C. W. de Jager, H. de Vries, A. Saha, and K. K. Seth, Phys. Lett. B **149**, 441 (1984).

[25] E. K. Warburton and B. A. Brown, Phys. Rev. C **43**, 602 (1991).

[26] M. Honma, T. Otsuka, B. A. Brown, and T. Mizusaki, Euro. Phys. J. A **25**, 499 (2005).

[27] B. A. Brown and W. A. Richter, Phys. Rev. C **74**, 034315 (2006).

[28] B. A. Brown and W. D. M. Rae, Nucl. Data Sheets **120**, 115 (2014). NUSHELLX provides reduced one-body density matrix elements (D_k) between the states. The occupations in Eq. (11) are related to these by $O_k = (\sqrt{2j+1}/\sqrt{2J+1})(D_k)$, where J is the spin of the nuclear state.

[29] J. Speth, L. Zamick, and P. Ring, Nucl. Phys. A **232**, 1 (1974).

[30] B. A. Brown and A. Schwenk, Phys. Rev. C **89**, 011307(R) (2014); **91**, 049902(E) (2015).

[31] R. F. Garcia Ruiz *et al.*, Nat. Phys. **12**, 594 (2016).

[32] D. M. Rossi, K. Minamisono, H. B. Asberry, G. Bollen, B. A. Brown, K. Cooper, B. Isherwood, P. F. Mantica, A. Miller, D. J. Morrissey, R. Ringle, J. A. Rodriguez, C. A. Ryder, A. Smith, R. Strum, and C. Sumithrarachchi, Phys. Rev. C **92**, 014305 (2015).